

## Supplementary information for

Atrophy in distinct corticolimbic networks predicts social impairments in frontotemporal dementia

Kevin C. Bickart<sup>1</sup>, Michael Brickhouse<sup>2,5</sup>, Alyson Negreira<sup>2,5</sup>, Daisy Sapolsky<sup>3,5</sup>, Lisa Feldman Barrett<sup>2,4\*</sup>, Bradford C. Dickerson<sup>2,5\*</sup>

<sup>1</sup>Department of Anatomy and Neurobiology, Boston University School of Medicine, <sup>2</sup>Psychiatric Neuroimaging Research Program and Martinos Center for Biomedical Imaging, Massachusetts General Hospital, <sup>3</sup>Department of Speech and Language Pathology, Massachusetts General Hospital, <sup>4</sup>Department of Psychology, Northeastern University, <sup>5</sup>Frontotemporal Disorders Unit, Department of Neurology, Massachusetts General Hospital and Harvard Medical School

Corresponding Author:  
Brad Dickerson, M.D.  
MGH Frontotemporal Disorders Unit  
149 13<sup>th</sup> Street, Suite 2691  
Charlestown MA 02129  
617-726-5571  
617-726-5760  
bradd@nmr.mgh.harvard.edu

### **This file includes:**

Supplementary METHODS  
Supplementary RESULTS  
Supplementary DISCUSSION  
Supplementary Tables 1-8  
Supplementary Figure 1

## SUPPLEMENTARY METHODS

### *MRI data acquisition*

MRI data were acquired using a Siemens Trio 3.0 Tesla scanner (Siemens Medical Systems, Erlangen, Germany), including an MPRAGE sequence (repetition time/inversion time/echo time 2,300/900/2.98 msec, field of view 256mm, flip angle 7°, 192 sagittal 1-mm-thick slices, matrix 240x256) and a FLAIR sequence, which was visually inspected to rule out non-neurodegenerative pathologies.

### *Subcortical MRI segmentation methods*

FreeSurfer 5.0 (<http://surfer.nmr.mgh.harvard.edu>) was used for all MRI data analysis. For subcortical segmentation, this method employs a manually labeled atlas dataset from 40 individuals to automatically segment and assign neuroanatomic ROI labels to 37 different brain structures based on probabilistic estimations. Using Bayesian statistics, the probability of the presence of a particular neuroanatomic structure at a particular location is estimated given the image intensity, the likelihood that a particular tissue class would be present at a given location, and the probability of a particular anatomic structure given the tissue types within a local area. This automated segmentation procedure has been widely used in volumetric studies and was shown to be comparable in accuracy to that of manual labeling (Fischl et al., 2002) and across sessions within the same scanner (Jovicich et al., 2009).

In the present study, each anatomic dataset was processed using the fully automated algorithm and then the subcortical segmentations of each subcortical ROI were manually verified. A trained operator, blind to the hypothesis, manually inspected the results of the automated segmentation. In this analysis, no adjustments, modifications, or edits were made; the results of the automated segmentation were verified as accurate without need for correction. The subcortical ROIs on which we focused in this study included the amygdala, hippocampus, nucleus accumbens, and putamen; for each structure, the volumetric measurement was obtained from the FreeSurfer output file and divided by total intracranial volume also obtained from the FreeSurfer output file.

### *Cortical Parcellation and Estimation of Cortical Thickness*

After spatial and intensity normalization and skull stripping, the resulting volume was then used to segment cerebral white matter (Dale et al., 1999) and locate the gray/white boundary. Defects in the surface topology were corrected (Fischl et al., 2001) and the gray/white boundary was deformed outward using an algorithm designed to obtain an explicit representation of the pial surface (Fischl and Dale, 2000). The cortical surface volume was manually edited to improve technical accuracy in accordance with standard, objective editing rules. In this study, minimal manual editing was required.

For the purposes of comparing cortical thickness measures across subjects, it is necessary to establish a common surface-based coordinate system. To achieve this, a spherical averaging method was used to normalize and align cortical folding patterns across subjects by morphing and registering each subject's reconstructed brain to an average spherical surface representation (Fischl et al., 1999a; Fischl et al., 1999b). Each subject's surface was then divided into cortical ROIs by labeling each of approximately 160,000 points per hemisphere based on 1) prior probability of that label matching a location on an atlas derived from a manually-parcellated training set, 2) local curvature information, and 3) information about the adjacent labels and folding patterns.

We obtained cortical thickness measures for 19 ROIs per hemisphere (see **Supplementary Table 1** for a list of ROIs) derived mostly from previously developed parcellation schemes (Desikan et al., 2006; Destrieux et al., 2010).

#### *Deriving new cortical labels*

For regions of interest that required different boundaries than those defined within the available parcellation schemes (Desikan et al., 2006; Destrieux et al., 2010) or in cases where the anatomical boundaries of ROIs from these schemes overlapped, we created new cortical labels. To do this, we manually drew new labels (indicated by *Bickart-Dickerson* in the Atlas column of **Supplementary Table 1**) or edited previously developed labels (indicated by an *asterisk\** in the Atlas column of **Supplementary Table 1**) in Freesurfer's *tksurfer* on an average surface created from 40 healthy subjects, as described in more detail below. The newly derived cortical labels were then mapped to each patient and control subject using Freesurfer's automated parcellation procedure described above.

*Dorsomedial prefrontal cortex.* We were interested in examining cortical thickness within a functional division of the medial prefrontal cortex implicated in mentalizing that lies dorsal to the ventromedial prefrontal cortex, often called the dorsomedial prefrontal cortex. To establish its boundaries, we referenced a meta-analysis of functional neuroimaging studies employing mentalizing tasks (Amodio and Frith, 2006), which delineated a swath of medial prefrontal cortex dorsal to the superior rostral gyrus, which extended to a vertical line rising perpendicularly from the rostral anterior cingulate cortex to the dorsomedial convexity of the superior frontal gyrus. Based on this meta-analysis, we created a cortical label for the dorsomedial prefrontal cortex by drawing a new label on the medial surface of the superior frontal gyrus using the anatomical boundaries of the medial orbitofrontal and anterior cingulate cortex labels of the Desikan-Killiany atlas (Desikan et al., 2006). The caudal boundary was a vertical line extending dorsally from the border between the rostral and caudal anterior cingulate cortex labels of the Desikan-Killiany atlas to the dorsomedial convexity of the superior frontal gyrus.

The label was limited dorsally and rostrally by a line following the dorsomedial convexity of the superior frontal gyrus rostro-ventrally to the level of the medial orbitofrontal cortex label of the Desikan-Killiany atlas (i.e., the superior rostral gyrus). The ventral and caudal boundaries were the medial orbitofrontal and rostral anterior cingulate cortex labels of the Desikan-Killiany atlas, respectively (see **Supplementary Figure 1** for a depiction of this label).

*Ventral and dorsal temporal poles.* We were also interested in delineating ventrolateral and dorsomedial divisions of the temporal pole based on functional and connectional grounds. The ventrolateral temporal pole has been implicated in multisensory integration (Zahn et al., 2007) and demonstrates preferential connectivity with Price and colleagues' orbital/sensory as compared to medial/visceromotor prefrontal network in monkeys (Saleem et al., 2008; Price and Drevets, 2010). The dorsomedial temporal pole is implicated in representing abstract person-specific semantic knowledge (Zahn et al., 2007) and demonstrates preferential connectivity with Price and colleagues' medial as compared to orbital prefrontal network in monkeys (Saleem et al., 2008; Price and Drevets, 2010). Based on these functional and connectional distinctions, we delineated ventrolateral and dorsomedial divisions of the temporal pole. The caudal boundary of both temporal pole divisions was a line encircling the temporal pole at a level just rostral to the temporal stem. The boundary delineating ventrolateral from dorsomedial divisions was a diagonal line extending from the rostral-most point of superior temporal sulcus across the temporal pole to the rostral-most point of the rhinal sulcus. Thus, the ventrolateral temporal pole label contained the rostral-most extension of the middle and inferior temporal gyri and fusiform gyrus whereas the dorsomedial temporal pole label contained the rostral-most extension of the superior temporal gyrus and entorhinal cortex. Because these new temporal pole labels overlapped to a small degree with the fusiform gyrus and entorhinal cortex labels of the Desikan-Killiany atlas, which were also ROIs in this study, we removed the rostral-most extension of the fusiform gyrus and entorhinal cortex labels to eliminate any anatomical overlap (see **Supplementary Figure 1** for a depiction of these labels).

*Lateral orbitofrontal cortex.* The boundaries of the lateral orbitofrontal cortex label from the Desikan-Killiany atlas and the anterior segment of the circular sulcus of the insula label of the Destrieux 2009 atlas, both ROIs in this study, overlapped to a small degree. We loaded these labels in Freesurfer's tksurfer on the average surface, fsaverage, and eliminated a patch of the lateral orbitofrontal cortex label in the caudal-most corner that overlapped with the anterior segment of the circular sulcus of the insula (see **Supplementary Figure 1** for a depiction of this label).

*Superior temporal sulcus.* We also divided the superior temporal sulcus from the Destrieux 2009 atlas into posterior and anterior segments (pSTS and STS, respectively) because the most

posterior segment has been implicated in the mirror network (Van Overwalle and Baetens, 2009). We used the posterior tip of the Sylvian fissure to demarcate the anterior extent of the pSTS (see **Supplementary Figure 1** for a depiction of this label).

## **SUPPLEMENTARY RESULTS**

### **Summary of social impairments assessed within each SIRS domain**

#### *Inappropriate trusting and approach behavior*

Scores in the SIRS domain, inappropriate trusting and approach behavior, reflect the severity of patients' impairment in judging the trustworthiness and approachability of other people especially strangers, salesmen, or solicitors. Based on caregiver reports, patients with higher scores in this domain became more extraverted and less cautious towards others where they would approach strangers on the street or in restaurants without restraint and strike up a conversation that was usually overly friendly or personally revealing (but not crude or rude). For example, one patient invited a stranger that she met in the neighborhood into her house to show the stranger her family photographs. Such patients also exhibited overly agreeable, gullible, and trusting behaviors towards others leading to increased vulnerability to very costly financial scams from solicitors over the phone or at the door as well as salesmen in stores and on television infomercials. For example, one patient gave away his and his wife's mobile home to a stranger for free. Another patient agreed to pay door-to-door roofers, who were later arrested for scamming several households, thousands of dollars to fix his roof and when his wife asked why he agreed to pay them he said, "They looked nice and it sounded like a good idea." Several patients who scored high in this domain also began to get involved with more deceptive and manipulative people who took advantage of the patients financially and, in one case, sexually. Examples of caregiver descriptions of how patients' trustworthiness judgments had changed from premorbid status include, "She is very free. No barriers. No gates.", "He meets them at a level that they are trustworthy without a doubt now.", and "She has no doubt that everyone in this world is trustworthy."

#### *Socioemotional detachment: Lack of awareness of others' thoughts and intentions and lack of empathy or warmth*

This combined domain represents the severity of impairment in patients' comprehension of friends' or loved ones' internal states like their thoughts, intentions, feelings, or needs as well as patients' initiation of warm or caring interpersonal behavior or tendency for indifferent or cold

interpersonal behavior. Based on caregiver reports, patients with higher scores in this combined domain exhibited almost no understanding of sarcasm, deception, irony, and humor or friends' or loved one's displays of distress, anger, or pain. They also no longer initiated and hardly reacted to acts of interpersonal warmth like hugs or kisses when greeting family or friends ("it was like hugging a tree" one caregiver said about a patient) nor comforted loved ones in distress [one caregiver described that the patient, "looked at him (son-in-law) as if confused why he would be crying even though his mother just died."]. Such patients no longer displayed helping behavior like carrying in the groceries, opening a door for another person, or tending to the needs of a sick or injured loved one (a caregiver explained that the patient "didn't even look at her granddaughter when she stubbed her toe and burst into tears."). Overall, caregivers described patients with higher scores in this combined domain as "emotionally detached or disconnected", "self-focused", or "indifferent towards others". Thus, we refer to this combined domain as socioemotional detachment.

#### *Lack of adherence to social norms*

Scores in the SIRS domain, lack of adherence to social norms, reflect the severity of patients' behavioral impropriety. Based on caregiver reports, patients who scored higher in this domain exhibited frequent, unrestrained crude, rude, jocular, aggressive, or criminal acts in public settings that were not easily redirected by the caregiver. For example, some patients who scored higher in this domain lost basic manners and hygiene at home and in public where they would eat from others' plates, pass gas and giggle, belch, spit, urinate in parking lots and gardens, or stop bathing. Patients who scored high in this domain also frequently made rude or sexually explicit remarks or jokes about or to others such as "I would really like to see her breasts.", "Oh he's just a self-important want-to-be. He's an old shit.", or "I'm glad I'm not as big as that man." Other patients who scored high in this domain have broken the law by opening others' mail, sexually harassing a coworker, breaking into women's homes to ask for sex, or violating multiple restraining orders.

#### *Lack of attention or response to social cues*

Scores in the SIRS domain, lack of attention to social cues, reflect the severity of patients' impairment in attending and responding to the physical gestures and expressions of others during social interactions. Based on caregiver reports, some patients who scored higher in this domain exhibited diminished spontaneous orienting of attention to the eye region of others' faces, their facial and head movements (e.g. raising of an eye brow or nodding of the head), or even exaggerated hand and arm gestures like pointing in the direction of an object or location. In these cases, caregivers could often get

patients' attention verbally but even that was more difficult than normal. Other patients who scored higher in this domain that did attend to physical gestures and expressions to some degree, but exhibited diminished sensitivity to these cues where they would continue speaking or interrupting despite another person's attempts to end the conversation, stand or lean too close to others without regard to personal boundaries, or fail to understand the meaning of basic gestures like head nods or hand-pointing.

### *Person recognition difficulty*

Scores in the SIRS domain, person recognition difficulty, reflect the severity of impairment in patients' ability to recognize familiar people and tendency to misrecognize strangers as familiar. Patients who scored higher in this domain only recognized the people that they saw most frequently and failed to recognize previous coworkers, acquaintances, distant relatives, and in some cases even close friends and family members, particularly if there had been a lapse in time since their last encounter. Other patients that scored higher in this domain frequently misrecognized strangers as someone they used to know. In these cases, patients were often so confident that it was a particular familiar person that they would engage in conversation with him/her. Caregivers reported that sometimes the misrecognized strangers resembled who the patient believed it to be and sometimes they did not.

### *Social withdrawal*

Scores in the SIRS domain, social withdrawal, reflect the severity of patients' disinterest and disengagement in social interactions. Patients who scored higher in this domain no longer initiated contact with friends or loved ones and exhibited diminished interest in conversations or engaging in any level of social interaction even if it was initiated by a friend or loved one. For example, patients who scored higher in this domain would prefer to play computer games or do puzzles by themselves over visiting with friends and family, fall asleep at the restaurant during lively discussion, turn down activities with their grandchildren, or seat themselves in the corner during holiday events. They also often needed to be convinced or forced to go to social events.

## **SUPPLEMENTARY DISCUSSION**

### **Additional discussion of the balance between social affiliation and aversion**

In the present study, some of the patients who demonstrated severe socioemotional detachment were not just indifferent to others but were frankly cold toward them or actively avoided spending time with them. Taken together with the finding that this symptom profile was explained more by atrophy in the

affiliation than aversion network suggests that perhaps these patients had severe dysfunction in the affiliation network with partially preserved function in the aversion network, tipping the finely sculpted balance between these networks. This notion is consistent with findings from a sample of patients with ventromedial prefrontal cortex damage who retained relatively normal social aversive responses to unfair offers (Koenigs and Tranel, 2007; Krajchich et al., 2009).

### **Neuroanatomic correlates of impaired norm-abiding social behavior**

Some patients in our study also displayed varying degrees of behavioral disinhibition such as crude, rude, and vulgar comments and behaviors in public as well as diminished manners and hygiene. Some of these patients also became hypersexual or committed criminal acts. Patients with the most severe *lack of adherence to social norms* demonstrated the most severe atrophy in the affiliation network.

This is consistent with previous studies of FTD patients that have also traced symptoms of behavioral disinhibition back to morphometric changes in structures spanning both aversion and affiliation networks (Rosen et al., 2005; Zamboni et al., 2008; Krueger et al., 2011). For example, two studies using the NPI to assess the degree of behavioral disinhibition both found disinhibition-related gray matter reductions in the medial and lateral sectors of the left and right orbitofrontal cortex including the frontoinsula region in the caudolateral orbital surface and aspects of the temporal lobe (Massimo et al., 2009; Krueger et al., 2011). One of these studies found additional correlations with the right rostral anterior cingulate cortex (Krueger et al., 2011). A third study demonstrated volume reductions within the amygdala, nucleus accumbens, hippocampus, and superior temporal sulcus in relation to FTD patients' degree of behavioral disinhibition as assessed by the Frontal Systems Behavioral Scale (Zamboni et al., 2008).

Focusing on specific regions, we found that atrophy in the left ventromedial prefrontal cortex explained the most variance in the severity of patients' *lack of adherence to social norms*. These findings are in close agreement with previous work in patients with focal lesions to the ventromedial prefrontal cortex who exhibit severe behavioral disinhibition and deficits in moral judgments and decisions in real-world and experimental settings (Hornak et al., 1996; Hornak et al., 2003). For example, a recent study examined moral judgment and decision-making abilities in patients with ventromedial prefrontal cortex lesions using a series of personal and impersonal moral dilemmas as well as non-moral dilemmas. Patients made decisions comparable to a sample of healthy controls on impersonal moral and non-moral dilemmas but approved a greater number of moral violations in personal moral dilemmas than controls (Ciaramelli et al., 2007). That is, these patients tended to treat personal and impersonal moral dilemmas similarly by making the utilitarian, or logical, choice for both types of dilemmas. FTD patients exhibit



the same bias in personal moral dilemmas whereby, for example, they choose to save more people at the expense of one person's life even if it requires causing direct harm to that person (Mendez et al., 2005; Mendez and Shapira, 2009).

Based on a recent review of impaired moral judgment and decision-making in FTD and ventromedial prefrontal cortex-damaged patients, Mendez (2009) proposed a model in which moral behavior relies on the ventromedial and orbitofrontal cortices, amygdala, as well as the anterior insula, temporal pole, ventral striatum, and posterior superior temporal sulcus. In this review, Mendez emphasizes a potential functional division of labor within this circuitry where the amygdala, orbitofrontal cortex, and anterior insula are important for evaluating social feedback, activating social aversion sentiments, and regulating impulsive behavior while the ventromedial prefrontal cortex and related reward and autonomic structures are important for prosocial sentiments and affiliative behaviors. Based on his model, Mendez hypothesized that if either of these functionally distinct networks is disrupted it could lead to inappropriate, or disinhibited, social approach or withdrawal behaviors. Our zero-order correlation results suggest that structures within both of these networks might play a role in regulating avoidant and affiliative tendencies in the service of norm-abiding behavior, but based on regression analyses, it appears that in our sample of FTD patients, atrophy in the affiliation network, and the ventromedial prefrontal cortex in particular, is the best predictor of disrupted norm-abiding behavior.

### **Rationale for choosing a mixed sample**

As in previous brain-behavior studies in frontotemporal dementia (C. E. Krueger, et al., 2011; W Liu, et al., 2004; Rankin, et al., 2006; Rankin, et al., 2009; H. J. Rosen, et al., 2005; Zamboni, et al., 2008; Brambati, et al., 2006; Sollberger, et al., 2009), we chose here to study a mixed sample with patients who have variable clinical phenotypes within the FTD spectrum and variable degrees and distributions of social cognitive impairment and gray matter atrophy. This choice was made, as in the previous studies and also as in studies of patients with focal brain lesions such as stroke (M. F. Schwartz, et al., 2009), to increase the power of the planned regression analyses. Nevertheless, this also presents a potential weakness in that differences observed in the types and severity of social impairment and brain atrophy could be due to differences inherent to the diagnostic subgroups. We specifically examined whether diagnosis had an effect on our variables of interest and found that although the PNFA subgroup had lower severity scores in the *socioemotional detachment* domain than the other groups, they were not statistical outliers and controlling for diagnostic group did not change our main findings. Thus, in our study, diagnostic subgroup did not seem to play an appreciable role in our results.

**Social withdrawal**

We believe that the SIRS domain, “social withdrawal”, captured two additional confounding symptom categories – apathy and language difficulties. That is, it was challenging for caregivers to distinguish between a specific lack of interest or withdrawal from social interaction and a more general lack of interest for all activities, or apathy. In addition, for the aphasic patients, it was challenging for the caregivers to distinguish between diminished interest in social interaction and a difficulty in communication. We speculate that this might be why there was not a correlation between the severity of “social withdrawal” and atrophy in one of our networks of interest.

**Supplementary Table 1.** Label names and sources of anatomical regions of interest for each network

Networks of interest	Regions of interest	Label name	Atlas
Perception network	Fusiform gyrus	Fusiform gyrus	Desikan-Killiany*
	Ventral temporal pole	--	Bickart-Dickerson
	Superior temporal sulcus	Superior temporal sulcus	Destrieux 2009*
	Lateral orbitofrontal cortex	Lateral orbitofrontal cortex and pars orbitalis	Desikan-Killiany*
Affiliation network	Ventromedial prefrontal cortex	Medial orbitofrontal cortex	Desikan-Killiany
	Subgenual anterior cingulate cortex	Subcallosal cortex	Destrieux 2009
	Rostral anterior cingulate cortex	Rostral anterior cingulate cortex	Desikan-Killiany
	Nucleus accumbens	Nucleus accumbens	FS Subcortical
	Hippocampus	Hippocampus	FS Subcortical
	Entorhinal cortex	Entorhinal cortex	Desikan-Killiany*
	Parahippocampus	Parahippocampus	Desikan-Killiany
	Dorsal temporal pole	--	Bickart-Dickerson
Aversion network	Ventral insula	Combined short and long gyri of insula	Destrieux 2009
	Frontoinsula	Anterior segment of the circular sulcus of the insula	Destrieux 2009
	Caudal anterior cingulate cortex	Caudal anterior cingulate cortex	Desikan-Killiany
	Putamen	Putamen	FS Subcortical
Mentalizing network	Temporoparietal junction	Angular gyrus	Destrieux 2009
	Dorsomedial prefrontal cortex	--	Bickart-Dickerson
	Posterior cingulate cortex	Posterior and isthmus divisions of the cingulate cortex	Desikan-Killiany
	Precuneus	Precuneus	Desikan-Killiany
Mirror network	Ventral premotor cortex	Pars opercularis	Desikan-Killiany
	Intraparietal sulcus	Intraparietal sulcus	Destrieux 2009
	Posterior superior temporal sulcus	Superior temporal sulcus	Destrieux 2009*

This table includes the names of the labels and atlases from which we derived each anatomical region of interest (ROI). Desikan-Killiany (Desikan et al., 2006) and Destrieux 2009 (Destrieux et al., 2009) atlases were used for the majority of cortical ROIs. Freesurfer's automated segmentation was used to label subcortical ROIs (indicated by FS Subcortical in the Table). In the Atlas column of the table, we

also denote cases where we created new ROIs (Bickart-Dickerson) or we edited existing ROIs so they did not overlap with new ROIs or ROIs from the other atlas (\*) using Freesurfer's tksurfer.

**Supplementary Table 2.** Demographic and clinical characteristics of patients.

	Diagnosis	Age, y	Gender	Education, y	CDR global	CDR-SB	FTLD- CDR	MMSE
Patient 1	PPA-S	61	M	20	0	0.0	0.5	28
Patient 2	bvFTD	65	M	12	0.5	2.5	0.5	25
Patient 3	PPA-S	53	F	18	0	0.5	0.0	27
Patient 4	bvFTD	59	M	14	0.5	3.0	0.5	29
Patient 5	PPA-G	50	F	16	0.5	1.0	0	30
Patient 6	bvFTD	53	F	18	0.5	2.0	1.0	27
Patient 7	bvFTD	71	F	18	0.5	3.5	2.0	28
Patient 8	bvFTD	74	M	16	1.0	4.5	1.0	29
Patient 9	bvFTD	59	F	17	0.5	3.0	1.0	17
Patient 10	PPA-S	61	F	16	1.0	7.5	2.0	21
Patient 11	bvFTD	71	F	18	0.5	3.5	1.0	26
Patient 12	bvFTD	70	F	16	1.0	4.0	0.5	25
Patient 13	PPA-G	58	M	12	0.5	3.5	0	26
Patient 14	PPA-G	68	F	20	0.5	1.0	0	28
Patient 15	bvFTD	62	F	18	0.5	1.5	1.0	29
Patient 16	bvFTD	58	M	18	0.5	2.5	1.0	26
Patient 17	bvFTD	58	M	20	1.0	4.0	2.0	20
Patient 18	bvFTD	64	F	16	1.0	5.5	2.0	23
Patient 19	bvFTD	65	F	11	1.0	5.5	2.0	5
Patient 20	bvFTD	77	M	16	0.5	4.0	1.0	29

Abbreviations: bvFTD, behavioral variant FTD; PPA-S, primary progressive aphasia- semantic type; PPA-G, primary progressive aphasia-agrammatic type; CDR, Clinical Dementia Rating scale; CDR-SB, CDR-Sum-of-Boxes; FTLD-CDR, CDR-Behavioral Comportment and Personality box; MMSE, Mini-Mental State Examination; – indicates that data were not available

**Supplementary Table 3.** Intraclass correlation coefficients (ICC) for inter- and intra-rater reliability of all SIRS domains scores using a two-way random effects model with absolute agreement

SIRS Domains	ICC	
	Inter-rater	Intra-rater
Lack of attention/ response to social cues	0.89**	0.94**
Inappropriate trusting and approach	0.95**	0.97**
Lack of adherence to social norms	0.90**	0.94**
Person recognition difficulty	0.71*	0.98**
Social withdrawal	0.89**	0.97**
Lack of empathy or warmth	0.90**	0.97**
Lack of awareness of others' thoughts	0.95**	0.99**

\*\* $p < 0.001$ ; \* $p < 0.01$

**Supplementary Table 4.** Correlation matrix between SIRS domain scores

	Lack of attention or response to social cues	Inappropriate trusting and approach	Lack of adherence to social norms	Person recognition difficulty	Social withdrawal	Lack of empathy or warmth	Lack of awareness of others' thoughts
Lack of attention or response to social cues							
Inappropriate trusting and approach	0.48*						
Lack of adherence to social norms	0.61**	0.61**					
Person recognition difficulty	0.45*	0.19	0.24				
Social withdrawal	0.42†	0.08	0.18	0.34			
Lack of empathy or warmth	0.64**	0.42†	0.65**	0.43†	0.32		
Lack of awareness of others' thoughts	0.53*	0.61**	0.62**	0.18	0.32	0.78**	
Socio- emotional detachment	0.62**	0.55*	0.67**	0.32	0.34	0.94**	0.95**

† $p < 0.10$ ; \* $p < 0.05$ ; \*\* $p < 0.01$  The shaded cells indicate the combined SIRS domain, *socioemotional detachment*, computed as the average of the domains, *lack of empathy or warmth* and *lack of awareness of others' thoughts*.

**Supplementary Table 5.** SIRS domain and summary scores for each patient

	Lack of attention to social cues	Socioemotional detachment	Inappropriate trusting and approach	Lack of adherence to social norms	Person recognition difficulty	Social withdrawal	SIRS SB
Patient 1	0.5	1.0	1.0	0.5	1.0	0.5	4.5
Patient 2	2.0	2.0	1.0	0.0	1.0	2.0	8.0
Patient 3	1.0	2.0	2.0	2.0	0.0	2.0	9.0
Patient 4	1.0	0.8	0.5	1.0	0.0	1.0	4.3
Patient 5	0.0	0.0	0.0	0.5	0.0	0.5	1.0
Patient 6	1.0	3.0	2.0	3.0	0.0	0.5	9.5
Patient 7	3.0	2.0	3.0	2.0	2.0	1.0	13.0
Patient 8	1.0	2.5	3.0	0.5	0.0	1.0	8.0
Patient 9	0.0	0.5	0.0	0.0	0.0	0.5	1.0
Patient 10	2.0	3.0	3.0	3.0	2.0	2.0	15.0
Patient 11	1.0	2.0	1.0	1.0	0.0	1.0	6.0
Patient 12	0.5	1.0	0.0	0.0	0.0	3.0	4.5
Patient 13	0.0	0.3	0.5	0.0	0.0	0.5	1.3
Patient 14	2.0	1.0	3.0	3.0	0.0	1.0	10.0
Patient 15	0.5	2.0	2.0	2.0	2.0	2.0	10.5
Patient 16	3.0	2.5	1.0	3.0	2.0	3.0	14.5
Patient 17	1.0	2.0	1.0	2.0	2.0	1.0	9.0
Patient 18	2.0	2.5	3.0	3.0	0.0	2.0	11.5
Patient 19	1.0	2.0	3.0	3.0	0.0	1.0	10.0
Patient 20	2.0	3.0	0.5	3.0	0.0	1.0	9.5



**Supplementary Table 6.** Descriptive statistics for atrophy Z scores in neural networks of interest

	<b>M</b>	<b>SD</b>	<b>Variance</b>	<b>Range</b>
Right perception network	1.34	1.73	2.98	6.83
Left perception network	1.47	1.54	2.38	5.63
Right affiliation network	1.03	1.21	1.47	3.91
Left affiliation network	1.22	1.13	1.27	4.34
Right aversion network	0.61	0.74	0.55	2.82
Left aversion network	1.07	0.71	0.50	2.86
Right mentalizing network	0.49	1.12	1.25	4.55
Left mentalizing network	0.60	0.92	0.85	3.68
Right mirror network	1.00	1.17	1.37	4.55
Left mirror network	0.94	1.01	1.02	3.69

**Supplementary Table 7.** Correlated atrophy between neural networks of interest

	Right perception network	Left perception network	Right affiliation network	Left affiliation network	Right aversion network	Left aversion network	Right mentalizing network	Left mentalizing network	Right mirror network	Left mirror network
Right perception network										
Left perception network	0.66**									
Right affiliation network	0.81**	0.50*								
Left affiliation network	0.64**	0.86**	0.74**							
Right aversion network	0.71**	0.39†	0.90**	0.61**						
Left aversion network	0.38†	0.81**	0.49*	0.84**	0.52*					
Right mentalizing network	0.31	-0.04	0.34	0.07	0.55*	0.07				
Left mentalizing network	0.09	0.28	0.05	0.31	0.19	0.40†	0.66**			
Right mirror network	0.13	0.16	0.15	0.17	0.39†	0.42†	0.69**	0.70**		
Left mirror network	0.01	-0.02	-0.04	-0.08	0.24	0.20	0.68**	0.64**	0.83**	

\* $p < 0.05$  (two-tailed); \*\* $p < 0.01$  (two-tailed)

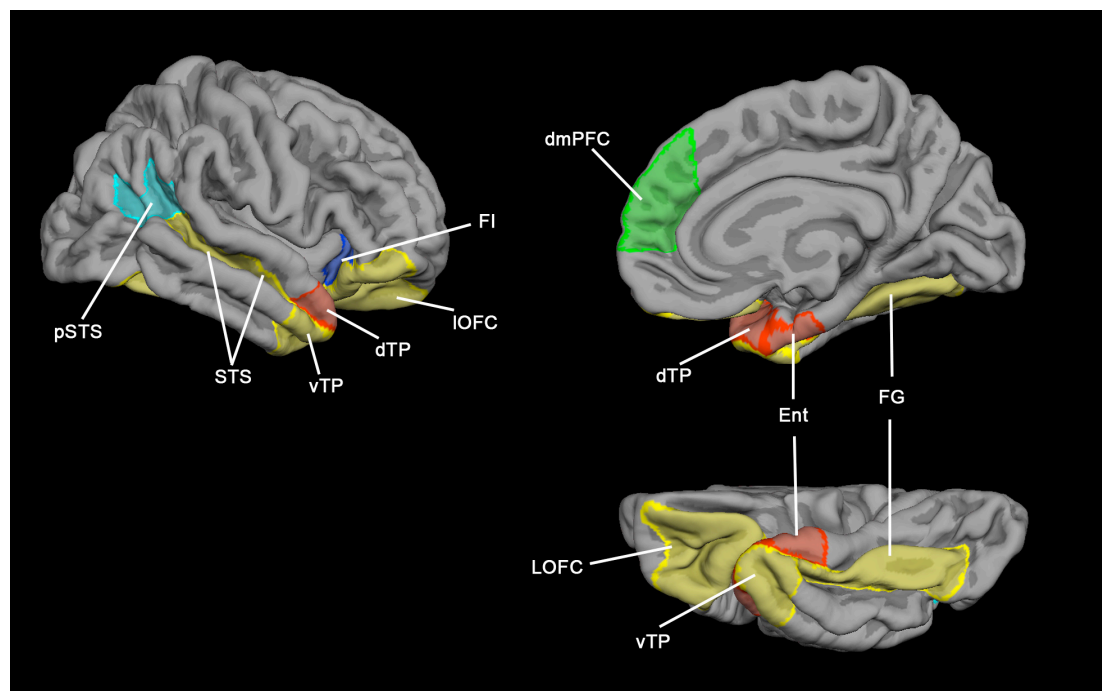
**Supplementary Table 8.** Associations between atrophy in individual ROIs and social impairment

	Atrophy in ROIs within each network	Lack of attention to social cues	Socio-emotional detachment	Inappropriate trusting and approach	Person recognition difficulty	Lack of adherence to social norms	SIRS sum-of-boxes score
	right amygdala	0.53*	0.58**	0.59**	0.29	0.43	0.60**
	left amygdala	0.39†	0.43†	0.43†	0.00	0.34	0.40†
Right perception network	lateral orbitofrontal cortex	0.12	0.18	0.33	0.38	0.20	0.24
	ventral temporal pole	0.57**	0.53*	0.44	0.40†	0.18	0.50*
	fusiform gyrus	0.57**	0.26	0.36	0.38†	0.01	0.37
	superior temporal sulcus	0.42†	0.17	0.17	0.61**	-0.11	0.28
	lateral orbitofrontal cortex	-0.12	0.26	0.57**	0.07	0.42†	0.27
Left perception network	ventral temporal pole	0.52*	0.41†	0.47*	0.25	0.20	0.42†
	fusiform gyrus	0.27	0.14	0.32	0.29	0.00	0.23
	superior temporal sulcus	0.12	0.07	0.37	0.27	0.02	0.18
	ventromedial prefrontal cortex	0.16	0.40†	0.30	0.23	0.26	0.32
Right affiliation network	subgenual anterior cingulate cortex	0.44	0.52*	0.49*	0.42†	0.34	0.56*
	rostral anterior cingulate cortex	0.21	0.41†	0.43†	0.15	0.52*	0.35
	dorsal temporal pole	0.58**	0.54*	0.45*	0.42†	0.19	0.52*
	hippocampus	0.53*	0.69**	0.51*	0.45*	0.39†	0.63**

Right affiliation network	entorhinal cortex	0.47*	0.57**	496*	0.35	0.28	0.53*
	parahippocampus	0.519*	0.66**	0.48*	0.50*	0.42†	0.63**
	nucleus accumbens	0.58**	0.74**	0.70**	0.20	0.58**	0.68**
	ventromedial prefrontal cortex	0.18	0.61**	0.65**	0.22	0.57**	0.57**
	subgenual anterior cingulate cortex	-0.05	0.46*	0.12	0.24	0.23	0.24
	rostral anterior cingulate cortex	0.16	0.22	0.27	0.38	0.40†	0.30
	dorsal temporal pole	0.56*	0.45*	0.44	0.22	0.35	0.49*
	hippocampus	0.45*	0.52*	0.58**	0.08	0.39†	0.51*
	entorhinal cortex	0.39†	0.52*	0.62**	0.23	0.35	0.50*
	parahippocampus	0.47*	0.46*	0.42†	0.19	0.21	0.40†
Left perception network	nucleus accumbens	0.35	0.66**	0.64**	0.20	0.53*	0.59**
	caudal anterior cingulate cortex	0.25	0.60**	0.39†	0.04	0.52*	0.47*
	frontoinsula	-0.11	0.00	0.41†	0.12	0.02	0.07
	ventral insula	0.42†	0.52*	0.58**	0.38†	0.42†	0.56*
	secondary somatosensory cortex	0.29	0.15	0.18	0.18	0.26	0.26
	putamen	0.46*	0.63**	0.60**	0.43†	0.44	0.62**

Left perception network	caudal anterior cingulate cortex	-0.34	-0.06	0.28	0.04	0.19	0.01
	frontoinsula	-0.08	0.23	0.47*	0.10	0.30	0.26
	ventral insula	0.03	0.29	0.61**	-0.15	0.26	0.23
	secondary somatosensory cortex	0.16	-0.10	0.17	0.03	0.03	0.02
	putamen	0.31	0.59**	0.58**	0.23	0.37	0.49*

**Supplementary Figure 1.** New cortical labels created or modified for this study.



## Supplementary REFERENCES

- Amodio DM, Frith CD (2006) Meeting of minds: the medial frontal cortex and social cognition. *Nat Rev Neurosci* 7:268-277.
- Ciaramelli E, Muccioli M, Ladavas E, di Pellegrino G (2007) Selective deficit in personal moral judgment following damage to ventromedial prefrontal cortex. *Soc Cogn Affect Neurosci* 2:84-92.
- Dale AM, Fischl B, Sereno MI (1999) Cortical surface-based analysis. I. Segmentation and surface reconstruction. *Neuroimage* 9:179-194.
- Desikan RS, Segonne F, Fischl B, Quinn BT, Dickerson BC, Blacker D, Buckner RL, Dale AM, Maguire RP, Hyman BT, Albert MS, Killiany RJ (2006) An automated labeling system for subdividing the human cerebral cortex on MRI scans into gyral based regions of interest. *Neuroimage* 31:968-980.
- Destrieux C, Fischl B, Dale A, Halgren E (2010) Automatic parcellation of human cortical gyri and sulci using standard anatomical nomenclature. *Neuroimage* 53:1-15.
- Fischl B, Dale AM (2000) Measuring the thickness of the human cerebral cortex from magnetic resonance images. *Proc Natl Acad Sci U S A* 97:11050-11055.
- Fischl B, Sereno MI, Dale AM (1999a) Cortical surface-based analysis. II: Inflation, flattening, and a surface-based coordinate system. *Neuroimage* 9:195-207.
- Fischl B, Liu A, Dale AM (2001) Automated manifold surgery: constructing geometrically accurate and topologically correct models of the human cerebral cortex. *IEEE Trans Med Imaging* 20:70-80.
- Fischl B, Sereno MI, Tootell RB, Dale AM (1999b) High-resolution intersubject averaging and a coordinate system for the cortical surface. *Hum Brain Mapp* 8:272-284.
- Fischl B, Salat DH, Busa E, Albert M, Dieterich M, Haselgrove C, van der Kouwe A, Killiany R, Kennedy D, Klaveness S, Montillo A, Makris N, Rosen B, Dale AM (2002) Whole brain segmentation: automated labeling of neuroanatomical structures in the human brain. *Neuron* 33:341-355.
- Hornak J, Rolls ET, Wade D (1996) Face and voice expression identification in patients with emotional and behavioural changes following ventral frontal lobe damage. *Neuropsychologia* 34:247-261.
- Hornak J, Bramham J, Rolls ET, Morris RG, O'Doherty J, Bullock PR, Polkey CE (2003) Changes in emotion after circumscribed surgical lesions of the orbitofrontal and cingulate cortices. *Brain* 126:1691-1712.
- Jovicich J, Czanner S, Han X, Salat D, van der Kouwe A, Quinn B, Pacheco J, Albert M, Killiany R, Blacker D, Maguire P, Rosas D, Makris N, Gollub R, Dale A, Dickerson BC, Fischl B (2009) MRI-derived measurements of human subcortical, ventricular and intracranial brain volumes: Reliability effects of scan sessions, acquisition sequences, data analyses, scanner upgrade, scanner vendors and field strengths. *Neuroimage* 46:177-192.
- Koenigs M, Tranel D (2007) Irrational economic decision-making after ventromedial prefrontal damage: evidence from the Ultimatum Game. *J Neurosci* 27:951-956.
- Krajchich I, Adolphs R, Tranel D, Denburg NL, Camerer CF (2009) Economic games quantify diminished sense of guilt in patients with damage to the prefrontal cortex. *J Neurosci* 29:2188-2192.
- Krueger CE, Laluz V, Rosen HJ, Neuhaus JM, Miller BL, Kramer JH (2011) Double dissociation in the anatomy of socioemotional disinhibition and executive functioning in dementia. *Neuropsychology* 25:249-259.

- Massimo L, Powers C, Moore P, Vesely L, Avants B, Gee J, Libon DJ, Grossman M (2009) Neuroanatomy of apathy and disinhibition in frontotemporal lobar degeneration. *Dement Geriatr Cogn Disord* 27:96-104.
- Mendez MF, Shapira JS (2009) Altered emotional morality in frontotemporal dementia. *Cogn Neuropsychiatry* 14:165-179.
- Mendez MF, Anderson E, Shapira JS (2005) An investigation of moral judgement in frontotemporal dementia. *Cogn Behav Neurol* 18:193-197.
- Price JL, Drevets WC (2010) Neurocircuitry of mood disorders. *Neuropsychopharmacology* 35:192-216.
- Rosen HJ, Allison SC, Schauer GF, Gorno-Tempini ML, Weiner MW, Miller BL (2005) Neuroanatomical correlates of behavioural disorders in dementia. *Brain* 128:2612-2625.
- Saleem KS, Kondo H, Price JL (2008) Complementary circuits connecting the orbital and medial prefrontal networks with the temporal, insular, and opercular cortex in the macaque monkey. *Journal of Comparative Neurology* 506:659-693.
- Van Overwalle F, Baetens K (2009) Understanding others' actions and goals by mirror and mentalizing systems: a meta-analysis. *Neuroimage* 48:564-584.
- Zahn R, Moll J, Krueger F, Huey ED, Garrido G, Grafman J (2007) Social concepts are represented in the superior anterior temporal cortex. *Proc Natl Acad Sci U S A* 104:6430-6435.
- Zamboni G, Huey ED, Krueger F, Nichelli PF, Grafman J (2008) Apathy and disinhibition in frontotemporal dementia: Insights into their neural correlates. *Neurology* 71:736-742.